

REVISITING PUTATIVE COOL ACCRETION DISKS IN ULTRALUMINOUS X-RAY SOURCES

J. M. MILLER¹, D. J. WALTON², A. L. KING¹, M. T. REYNOLDS¹, A. C. FABIAN³, M. C. MILLER⁴, AND R. C. REIS¹

¹ Department of Astronomy, University of Michigan, 500 Church Street, Ann Arbor, MI 48109-1042, USA; jonmm@umich.edu

² Cahill Center for Astronomy and Astrophysics, California Institute of Technology, Pasadena, CA 91125, USA

³ Institute of Astronomy, University of Cambridge, Madingley Road, Cambridge CB3 0HA, UK

⁴ Department of Astronomy, University of Maryland, College Park, MD 20742, USA

Received 2013 May 17; accepted 2013 September 16; published 2013 October 7

ABSTRACT

Soft, potentially thermal spectral components observed in some ultra-luminous X-ray sources (ULXs) can be fit with models for emission from cool, optically thick accretion disks. If that description is correct, the low temperatures that are observed imply accretion onto “intermediate-mass” black holes. Subsequent work has found that these components may follow an inverse relationship between luminosity and temperature, implying a non-blackbody origin for this emission. We have re-analyzed numerous *XMM-Newton* spectra of extreme ULXs. Crucially, observations wherein the source fell on a chip gap were excluded owing to their uncertain flux calibration, and the neutral column density along the line of sight to a given source was jointly determined by multiple spectra. The luminosity of the soft component is found to be positively correlated with temperature, and to be broadly consistent with $L \propto T^4$ in the measured band pass, as per blackbody emission from a standard thin disk. These results are nominally consistent with accretion onto black holes with masses above the range currently known in Galactic X-ray binaries, though there are important caveats. Emission from inhomogeneous or super-Eddington disks may also be consistent with the data.

Key words: accretion, accretion disks – black hole physics

Online-only material: color figure

1. INTRODUCTION

Ultra-luminous X-ray sources (ULXs) are variable, off-nuclear X-ray sources in nearby galaxies, with luminosities in excess of $L \simeq 10^{39}$ erg s⁻¹ (the Eddington luminosity of an $M = 10 M_{\odot}$ black hole). Though they are luminous, most ULXs are likely familiar objects. The well-known source GRS 1915+105, for instance, can be modestly super-Eddington for its mass, depending on the model and energy band considered. The vast majority of ULXs only exceed $L \simeq 10^{39}$ erg s⁻¹ by a small margin (Swartz et al. 2011; for a recent review, see Feng & Soria 2011).

The small subset of ULXs with luminosities of $L \simeq 10^{40}$ erg s⁻¹ and above are potentially more interesting, as they might be powered by accretion onto so-called intermediate-mass black holes (IMBHs), or an accretion flow that has genuinely defeated the isotropic Eddington limit. Of course, this small sub-class could be a combination of these two phenomena. An alternative possibility is that the emission from such sources is actually anisotropic, perhaps owing to a “funnel” in the inner accretion disk (King et al. 2001).

XMM-Newton has revolutionized studies of ULXs, making it possible to obtain spectra that require multiple components. Early efforts to decompose the best ULX spectra found evidence of separate soft and hard components. The soft components could be fit with disk models, and low temperatures obtained—generally $kT = 0.2$ – 0.3 keV—provided some evidence of accretion onto IMBHs since $T \propto M_{\text{BH}}^{-1/4}$ and $kT = 1$ keV is typical for accretion onto stellar-mass black holes close to the Eddington limit (e.g., Miller et al. 2003, 2004). This spectral decomposition is based on a close analogy with better-known X-ray binaries and may not be unique nor appropriate for ULXs. However, subsequent studies of soft component variability found that these would-be disks may not be blackbody-like

(Kajava & Poutanen 2009; Feng & Kaaret 2007, 2009; also see Soria 2007). Other recent work has discovered a spectral roll-over above the Fe *K* band (Gladstone et al. 2009). This can be interpreted as evidence of super-Eddington accretion, though the spectra still require independent soft components with low characteristic temperatures. In this work, we examine the nature of the best ULX spectra from nearby sources with $L \simeq 10^{40}$ erg s⁻¹, factoring in recent studies that impact the possibility of winds and variable absorption.

2. SAMPLE AND DATA REDUCTION

We considered the sample of nearby $L \simeq 10^{40}$ erg s⁻¹ sources observed with *XMM-Newton* and reported in Miller et al. (2004), Gladstone et al. (2009), and Kajava & Poutanen (2009). ULXs at distances greater than 5 Mpc were not considered owing to their reduced photon flux. Of the remaining sources, NGC 1313 X-2 was not considered as any evidence that it exceeds $L = 10^{40}$ erg s⁻¹ appears weak and highly model-dependent, and evidence for a cool disk component is only marginal (e.g., Miller et al. 2003). IC 342 X-1—which is near to $L = 10^{40}$ erg s⁻¹—was excluded owing to the modest significance of a putative cool component. In exploratory fits, the column density along the line of sight to IC 342 X-1 fell in the $N_{\text{H}} = 0.5$ – 1.5×10^{22} cm⁻² range, greatly complicating the detection of $kT \simeq 0.2$ keV emission. With these constraints, our sample includes Holmberg IX X-1, NGC 1313 X-1, Ho II X-1, NGC 5408 X-1, and NGC 5204 X-1. All archival *XMM-Newton* observations of these sources were downloaded and reduced using SAS version 12.0.1.

The EPIC-pn camera has the highest collecting area across the full 0.3–10.0 keV band, and is best calibrated for spectral fitting. For simplicity and self-consistency, our analysis was restricted to spectra obtained using the EPIC-pn camera. Unlike *Chandra*, *XMM-Newton* does not dither, and when a source

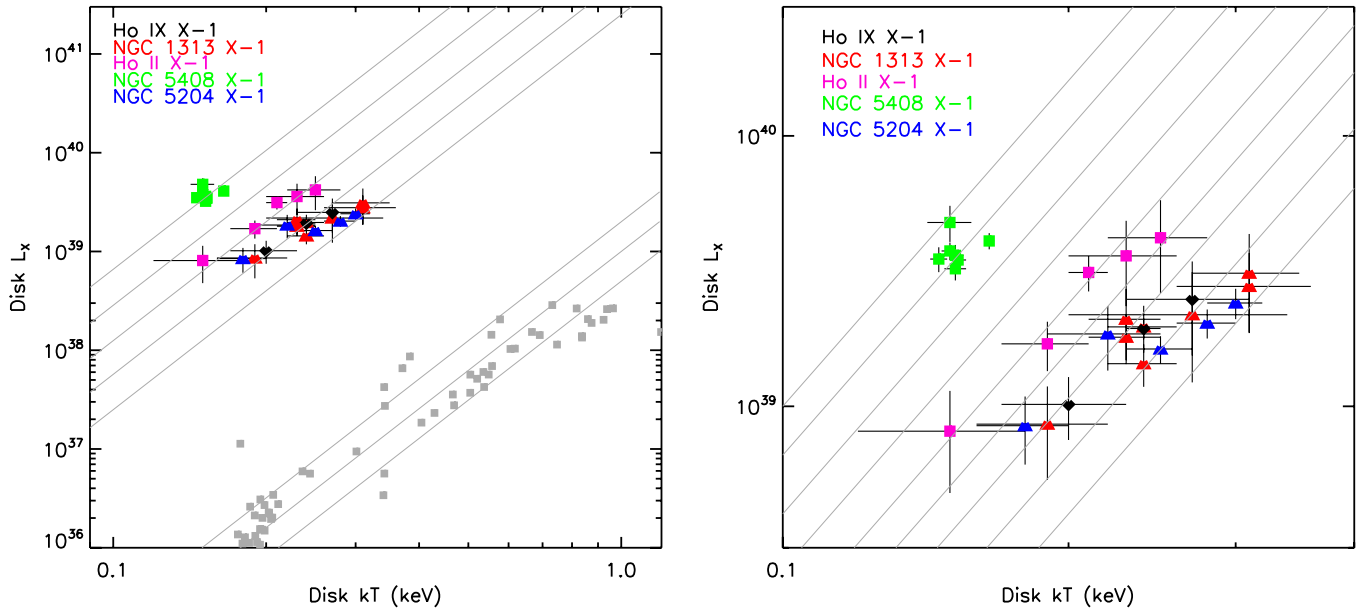


Figure 1. Figure above shows the luminosity of putative cool disk components vs. their apparent temperature, as measured in numerous spectra of ULXs with a total luminosity frequently in excess of $L \simeq 10^{40}$ erg s $^{-1}$. For comparison, data from a survey of stellar-mass black holes with *Swift* (Reynolds & Miller 2013; LMC X-3, GRS 1915 + 105, GX 339–4, XTE J1752–223, and XTE J1817–330 are shown) are plotted in gray in the left-hand panel. The diagonal gray lines depict $L \propto T^4$ with different normalizations. As these sources are not expected to have exactly the same mass, there is no reason to expect that they should follow $L \propto T^4$ with a common normalization. The left-hand and right-hand panels show the same ULX data; the right-hand panel merely examines a narrower range in L and kT . (A color version of this figure is available in the online journal.)

lands within the gap between chips in EPIC cameras, its effective exposure and encircled energy fraction can be affected, ultimately compromising flux estimates. Observations wherein the source image fell within chip gaps were therefore rejected, in order to ensure robust flux determinations.

Background regions were extracted on the same CCD as the source, and generally using an extraction region of the same size. The background regions were analyzed to identify periods of background flaring, and to create a GTI file to exclude these intervals when extracting events for spectral analysis. Spectra, backgrounds, and responses were then calculated using the appropriate tools. All spectra were grouped to require at least 25 counts bin $^{-1}$ using the FTOOL “grppha,” in order to ensure the validity of χ^2 statistical tests.

3. ANALYSIS AND RESULTS

All spectra were fit using XSPEC version 12.2 (Arnaud & Dorman 2000). Neutral interstellar absorption was fit using the “tbabs” model. As required by “tbabs,” the “vern” atomic cross-sections and “wilm” elemental abundances were used. The Milky Way’s contributions to the total neutral column density along these lines of sight are small, and we therefore used a single “tbabs” component to account for both Galactic absorption and the column within each ULX host galaxy. Solar abundances were assumed in all fits (but see the Discussion).

The spectral resolution afforded by dispersive spectrometers has recently been leveraged to address the extent to which absorption may drive spectral evolution in accreting systems (Miller et al. 2009). The depth of individual photoelectric absorption edges remains remarkably constant across a broad range in luminosity in low-mass X-ray binaries, in binaries with potential “intermediate-mass” stars such as Cygnus X-2, and even in Cygnus X-1 (which accretes from an O 9.7 Iab supergiant). This argues that the line of sight column density

should be held constant in spectral fits. Current limits on Fe K emission and absorption lines in ULXs are commensurate with detections in Galactic X-ray binaries, and far below expectations if line strengths scale with the mass accretion rate (Walton et al. 2012, 2013). We therefore fit all EPIC-pn spectra of a given ULX jointly, such that the interstellar column density was jointly determined and had a common value for every spectrum.

For simplicity, we chose to fit the soft, potentially thermal components with the well-known “diskbb” model (Mitsuda et al. 1984). To characterize the hard flux in each ULX spectrum, we used the “compTT” model (Titarchuk 1994). The use of “compTT” is important for characterizing the turn-over seen in the 6–10 keV band in many sensitive spectra of ULXs with $L \simeq 10^{40}$ erg s $^{-1}$ (e.g., Gladstone et al. 2009; Walton et al. 2013). It produced statistically superior fits to simple power-law models for the hard flux. The temperature of the low-energy thermal distribution T_0 was linked to that of the disk component. The other crucial parameters within “compTT,” the electron temperature kT_e and the optical depth τ were allowed to vary. However, few spectra are able to constrain both parameters, and in those cases a value of $kT_e = 2.0$ keV was adopted. This value is broadly consistent with the spectra where constraints were possible, and also broadly consistent with the values reported in fits with “compTT” reported by Gladstone et al. (2009) and Feng & Kaaret (2009).

An additional diffuse emission component is present in the spectra of NGC 5408 X-1, likely due to local warm gas and star formation. Emission localized around 1 keV can be modeled with a “mekal” plasma with $kT = 0.87(2)$ keV and a normalization of $8.0 \pm 0.5 \times 10^{-5}$. These values were determined through joint fits. This correctly accounts for diffuse emission with a constant flux.

The results of our spectral fits are given in Table 1. The procedure of jointly determining the column density is clearly one that allows for excellent fits. In all cases, the joint fit returns

Table 1
Spectral Fitting Results

Source	ObsID	N_H (10^{22} cm^{-2})	kT (keV)	Norm.	kT_e (keV)	τ	Norm (10^{-4})	L_{tot} ($10^{40} \text{ erg s}^{-1}$)	L_{disk} ($10^{39} \text{ erg s}^{-1}$)	χ^2/ν
Ho IX X-1	0112521001	0.157(7)	0.27(4)	20(7)	2.8(5)	7.2(9)	7.6(9)	1.3(5)	2.5(9)	2139.9/2140
	0112521101		0.20(3)	28(6)	5.7(2)	4.4(2)	6.1(4)	1.4(4)	1.0(3)	
	0200980101		0.24(1)	26(2)	2.45(8)	8.9(3)	7.2(2)	1.1(1)	1.9(2)	
NGC 1313 X-1	0106860101	0.272(8)	0.24(2)	28(5)	2.3(3)	8.5(7)	4.2(3)	0.6(1)	2.0(4)	2513.8/2398
	0150280201		0.24(2)	19(3)	2.0	10(3)	6(3)	0.5(1)	1.4(3)	
	0150280601		0.31(4)	16(6)	2.0	7.5(5)	7(1)	0.9(3)	3(1)	
	0150281101		0.27(7)	17(6)	2.0	6.6(3)	10(4)	0.9(3)	2(1)	
	0205230201		0.31(5)	14(4)	2.0	9(1)	4(1)	0.7(2)	2.8(9)	
	0205230401		0.19(3)	32(9)	2.0	4.2(2)	10(3)	0.5(1)	0.8(3)	
	0205230601		0.23(3)	32(9)	2.0	8.7(4)	5.4(5)	0.7(2)	2.1(5)	
	0405090101		0.23(2)	27(5)	2.2(2)	8.5(5)	4.3(1)	0.6(1)	1.8(3)	
Ho II X-1	0112520601	0.080(3)	0.25(3)	70(25)	2.0	5.9(3)	12(3)	1.1(4)	4(2)	2033.6/1990
	0112520701		0.23(3)	60(20)	2.0	6.6(3)	11(3)	1.0(4)	4(1)	
	0112520901		0.15(3)	140(50)	2.0	4.8(3)	6(3)	0.3(1)	0.8(3)	
	0200470101		0.21(1)	85(12)	2.7	4.6(6)	13(1)	1.2(2)	3.1(5)	
	0561580401		0.19(2)	84(15)	2.0	5.6(3)	6.4(6)	0.46(9)	1.7(4)	
NGC 5408 X-1	0112290501	0.105(3)3	0.150(8)	350(50)	2.0	5.0(3)	6(1)	1.0(2)	4.8(7)	3686.4/3551
	0302900101		0.165(3)	177(12)	2.0	5.1(2)	4.1(3)	0.72(7)	4.1(3)	
	0500750101		0.152(4)	220(20)	2.0	5.57(9)	4.9(3)	0.67(7)	3.2(3)	
	0653380201		0.150(3)	280(20)	2.0	5.5(1)	6.5(3)	0.83(7)	3.8(3)	
	0653380301		0.146(3)	290(30)	2.0	5.30(5)	6.9(4)	0.8(1)	3.5(4)	
	0653380401		0.152(3)	242(22)	2.0	5.42(6)	5.7(3)	0.78(8)	3.6(4)	
	0653380501		0.153(3)	220(20)	2.0	5.58(6)	5.5(2)	0.75(7)	3.5(3)	
NGC 5204 X-1	0142770101	0.049(4)	0.18(2)	27(7)	2.0	7.6(3)	3.2(5)	0.4(1)	0.9(2)	1634.4/1601
	0142770301		0.28(2)	9.0(9)	2.0	8.1(8)	2.3(4)	0.5(1)	2.0(3)	
	0405690101		0.21(3)	27(6)	2.0	5.8(3)	6(1)	0.7(2)	1.8(5)	
	0405690201		0.30(2)	9(1)	2.0	6.8(3)	2.8(4)	0.6(1)	2.4(3)	
	0405690501		0.25(2)	12(1)	2.0	7.7(3)	2.7(3)	0.47(7)	1.6(2)	

Notes. The table above lists the results of joint spectral fits to the sources and observations in our sample, over the 0.3–10.0 keV range. The column density N_H was jointly determined. Where errors are not given, the parameter was fixed (see the text). In calculating luminosity values we assumed distances of 3.6 Mpc, 3.7 Mpc, 3.4 Mpc, 4.8 Mpc, and 4.3 Mpc for Ho IX X-1, NGC 1313 X-1, Ho II X-1, NGC 5408 X-1, and NGC 5204 X-1, respectively (Paturol et al. 2002; Tully 1988; Karachentsev et al. 2002).

a reduced χ^2 statistic that is close to unity. The use of the “compTT” component with a turn-over above the Fe K band also contributed to the excellent fits. Figure 1 plots the X-ray luminosity measured in the putative disk components, versus their color temperature values. Both in Table 1 and Figure 1, the luminosity is restricted to the band in which the flux was actually observed (0.3–10.0 keV).

Figure 1 also plots the relationship expected for simple blackbody emission, with a number of different normalizations. It is immediately apparent that the ULX putative disk components show a clear, positive relationship between luminosity and temperature that is qualitatively consistent with $L \propto T^4$. (Note that band pass effects can be important in effective luminosity versus temperature relationships; it is possible that $L \propto T^5$ may be anticipated for very cool disks measured in the 0.3–10.0 keV band.) The lone exception is NGC 5408 X-1; the points from that source are tightly clustered.

In order to quantify the apparent relationships, we ran statistical correlation tests on the data from each individual source, and also made simple least-squares fits to determine the slope of the data. The results of these tests and fits are listed in Table 2. Errors on both luminosity and temperature were considered in fitting the data and estimating errors on the slope. Strong positive correlations are confirmed in each source, apart from NGC 5408 X-1. The data from Ho IX X-1

Table 2
Correlation Tests and Fits

Source	ρ	P_{FA}	τ	P_{FA}	Index
Ho IX X-1	1.0	0.0	1.0	0.117	3.2 ± 2.6
Ho II X-1	1.0	0.0	1.0	0.014	3.7 ± 1.8
NGC 1313 X-1	0.84	0.0096	0.718	0.0129	2.4 ± 1.0
NGC 5408 X-1	-0.09	0.846	-0.05	0.8745	1.7 ± 0.9
NGC 5204 X-1	0.9	0.037	0.8	0.05	1.9 ± 0.6

Notes. The table above lists the results of correlation tests of putative disk temperature kT and luminosity L_{disk} , for the values given in Table 1. The Spearman’s rank correlation coefficient ρ and Kendall’s τ coefficients and their associated false alarm probabilities (probability of false correlation) are given. The index reported in the last column is the slope obtained in least-squares fits to the L_{disk} and kT data from each individual source. For simple blackbody emission, $L \propto T^4$ is expected, corresponding to an index of 4.0 in the final column.

and Ho II X-1 are formally consistent with $L \propto T^4$, and the slope of NGC 1313 X-1 is consistent within 1.5σ . The slope of NGC 5204 X-1 is somewhat flatter. The best traces of L versus kT in stellar-mass black hole disks—made using *Swift*, spanning three orders of magnitude in L , and also obtained using “diskbb” and “compTT” continuum components—find

more shallow slopes, e.g., $L \propto T^{3.3 \pm 0.1}$ (Rykoff et al. 2007; also see Reynolds & Miller 2013; Salvesen et al. 2013).

The errors on the slopes listed in Table 2 are large owing to the small number of points available. Similarly, the strongest correlations are only significant at the 99% level of confidence. However, taken literally, the data would suggest that the putative cool thermal disk components in this small subset of extreme ULXs may indeed represent disk emission. Since disk temperatures this low are only seen in stellar-mass black holes at or below $0.01 L_{\text{Edd}}$, the results would nominally indicate accretion onto more massive black holes, since $T \propto M_{\text{BH}}^{-1/4}$ for black hole accretion.

4. DISCUSSION AND CONCLUSIONS

We have examined the relationship between the color temperature of putative cool, thermal components versus their luminosity, in the 0.3–10.0 keV spectra of ULXs with $L_{\text{tot}} \simeq 10^{40}$ erg s⁻¹. We find evidence of positive correlations between the luminosity of these putative disk components, and their color temperature. In the observed band, some temperature and luminosity trends are formally consistent with the $L \propto T^4$ relationship expected for simple blackbody emission from a standard thin accretion disk. In all but one source, the data are consistent with a slightly flatter relationship that is observed in stellar-mass black holes in the same band (e.g., $L \propto T^{3.3 \pm 0.1}$; Rykoff et al. 2007; also see Reynolds & Miller 2013; Salvesen et al. 2013). The lone exception is NGC 5408 X-1, for which the data span a very small range in luminosity and temperature, and thus no trend can be discerned. Taken literally, these results may support an interpretation of these components as emission from cool accretion disks around IMBHs. We therefore proceed to make a critical examination of our methods and assumptions in this section.

As noted previously, some recent work has found putative disk luminosity and temperature to be anti-correlated when fitting ULX spectra with disk components at low energy (e.g., Feng & Kaaret 2007, 2009; Kajava & Poutanen 2009). Our analysis employed a more restrictive selection criterion, in that observations wherein the source image landed on a chip gap were excluded. Observations with spurious or uncertain flux measurements are therefore omitted. Moreover, the correlation we have found is specific: the *disk* luminosity and the *disk* temperature are positively correlated. We do not find strong correlations between *total* luminosity and disk temperature. Though coronae and disks must be linked, the need for magnetic processes (see, e.g., Merloni & Fabian 2001) means that the luminosity of these components can be decoupled at times.

Our analysis also differs from prior efforts in that the column density along the line of sight to a given source was jointly determined by the numerous spectra, and not allowed to vary between them. It is possible that this method is faulty, especially if ULXs are fueled by massive stars with variable, clumpy winds. However, existing data appear to justify our assumptions and fitting methods.

First, grating spectra of even Cygnus X-1 find a consistent column across the binary phase, except perhaps when the O star is closest to our line of sight (Miller et al. 2009). Second, existing spectra of NGC 1313 X-1 and Holberg IX X-1 now place extremely restrictive limits on emission and absorption features in these sources (Walton et al. 2013). Any emission lines must have lower equivalent widths than the lines seen in Galactic X-ray binaries with massive companions. This indicates that

companion winds are largely absent or very highly ionized. Either way, companion winds are unlikely to contribute to an evolving neutral column density. Limits on absorption lines are also below those detected from disk winds in stellar-mass black holes and many active galactic nuclei, again limiting the scope for variable absorption (Walton et al. 2012, 2013; Pasham & Strohmayer 2013). Last, where dips are detected in ULXs (e.g., NGC 5408 X-1; Grisé et al. 2013), they are apparently quasi-periodic (Pasham & Strohmayer 2013), and thus inconsistent with clumps in a companion wind. Dips in Cygnus X-1 are clustered at $\phi = 0.95$ and $\phi = 0.6$, with those at $\phi = 0.6$ likely due to the accretion stream impacting the outer disk; dips owing to clumps in the companion wind appear to be spread randomly in phase (Balucinska-Church et al. 2000). And, as noted previously, even in Cygnus X-1, the optical depth in various edges is remarkably constant (e.g., Miller et al. 2009).

In our treatment of the neutral column, we also assumed solar abundances for all elements. Some studies of the dwarfs in this sample (in particular) have reported sub-solar metallicity values in the inter-stellar medium of those galaxies (e.g., Guseva et al. 2011; Egorov et al. 2013), and caution is warranted. Fits to the best X-ray spectra, however—including gratings spectra obtained with the reflection grating spectrometer—find abundances consistent with solar (Winter et al. 2007; Pintore & Zampieri 2012). The same effect is found in our data: if the absorption model for Ho II X-1 in Table 1 is altered so that the metal abundances are only 10% of solar, a significantly worse fit is achieved ($\Delta\chi^2 = 44$). The same effect holds for the large spiral NGC 1313 ($\Delta\chi^2 = 132$). Such results are not driven by contributions from the Galactic column; in all cases, the Galactic column (as estimated by Dickey & Lockman 1990) is only a fraction of that measured. Moreover, it is important to remember a basic facet of the observed absorption edge features: one can trade intrinsic column density and abundance, but their product has to match the observed edge depth. Shifting abundance values will affect all spectra from a given source in the same manner.

The spectral model we employed also has difficulties. The “comptt” model includes thermal emission, and it therefore competes with the external “diskbb” component for the soft X-ray flux. In this sense, it is not perfectly self-consistent. However, “comptt” is required to describe the roll-over in the 5–10 keV band (e.g., Gladstone et al. 2009), and this is now a standard model. Alternative Comptonization treatments, such as “simpl,” only produce a power-law and thus miss the observed roll-over. For the fits presented in Table 1, the additional soft component is required by the data at extremely high statistical significance.

There are important caveats, but our results nominally support the possibility that soft components in ULX spectra represent emission from standard accretion disks extending to the ISCO. It is possible to derive some simple mass estimates by scaling from stellar-mass black holes: $M_{\text{ULX}} \simeq (M_{\text{XRB}}/M_{\odot}) \times (T_{\text{XRB}}/T_{\text{ULX}})^4$, where T_{XRB} is the disk temperature typical for stellar-mass black holes in X-ray binaries close to the Eddington limit (or, in a state analogous to that in which ULXs accrete). If we take $kT_{\text{XRB}} = 1$ keV, $M_{\text{XRB}} = 10 M_{\odot}$, $T_{\text{ULX}} = 0.2$ keV, then a mass of $M_{\text{ULX}} = 6250 M_{\odot}$ is implied. However, not all transients that cycle through each of the canonical spectral states are observed to have maximum temperatures of $kT \simeq 1$ keV. XTE J1650–500, for instance, had a maximum temperature of $kT \simeq 0.6$ keV (e.g., Reis et al. 2013). For $kT_{\text{XRB}} = 0.5$ keV, $M_{\text{XRB}} = 5 M_{\odot}$, and $kT_{\text{ULX}} = 0.25$ keV, a more modest mass

of $M_{\text{ULX}} \simeq 80 M_{\odot}$ is implied. Clearly, the mass estimate is strongly dependent upon the “typical” temperature of a standard X-ray binary disk at Eddington.

These mass estimates are simplified. There is no certainty that ULXs radiate at Eddington. Moreover, the data allow for flatter relationships between luminosity and temperature, potentially suggestive of a changing disk radius. In this circumstance, and in situations where the coronal energy drains the disk, mass estimates are more complex, and generally imply lower masses ($M_{\text{ULX}} \leq 100 M_{\odot}$; Soria 2007). The putative cool disk components in our models only emit a fraction of their luminosity in the observed (0.3–10.0 keV) band. However, these disks would dominate the source luminosity in the 0.01–10.0 keV band, and would then be more analogous with the disk-dominated “high/soft” states seen in stellar-mass black holes. Depending on numerous details, the slopes measured when considering bolometric disk luminosity versus temperature may be 0.5–1.0 flatter than the values reported in Table 2. This effect is within the error ranges quoted in the existing fits, and assumes that the spectral model can safely be extrapolated to lower energy values.

It is possible that the observed temperatures and flux trends could represent emission from a locally inhomogeneous disk, although the observed temperature contrast is slightly greater than that envisioned in current treatments (e.g., Dexter & Quataert 2012). It is also possible that the putative cool disk components we have studied do not originate close to the black hole, but rather outside of some transition radius, with an hot, inner, super-Eddington disk represented by the Comptonized component. In this scenario, however, considerable fine-tuning would likely be required for the different sources and transition radii to create the observed temperatures and trends. Future monitoring campaigns aimed at improved traces of soft component variability, and very deep observations that search for the outflows expected in super-Eddington regimes, may help to better understand this subset of ULXs.

REFERENCES

- Arnaud, K. A., & Dorman, B. 2000, XSPEC, <https://heasarc.gsfc.nasa.gov/docs/xanadu/xspec/>
- Balucinska-Church, M., Church, M. J., Charles, P. A., et al. 2000, *MNRAS*, **311**, 861
- Dexter, J., & Quataert, E. 2012, *MNRAS*, **426**, L17
- Dickey, J. M., & Lockman, F. J. 1990, *ARA&A*, **28**, 215
- Egorov, O. V., Lozinskaya, T. A., & Moiseev, A. V. 2013, *MNRAS*, **429**, 1450
- Feng, H., & Kaaret, P. 2007, *ApJL*, **660**, L113
- Feng, H., & Kaaret, P. 2009, *ApJ*, **696**, 1712
- Feng, H., & Soria, R. 2011, *NewAR*, **55**, 166
- Gladstone, J. C., Roberts, T. P., & Done, C. 2009, *MNRAS*, **387**, 1836
- Grisé, F., Kaaret, P., Corbel, S., Cseh, D., & Feng, H. 2013, *MNRAS*, **433**, 1023
- Guseva, N. G., Izotov, Y. I., Stasinska, G., et al. 2011, *A&A*, **529**, 149
- Kajava, J. J. E., & Poutanen, J. 2009, *MNRAS*, **398**, 1450
- Karachentsev, I. D., Sharina, M. E., Dolphin, A. E., et al. 2002, *A&A*, **385**, 21
- King, A. R., Davies, M. B., Ward, M. J., Fabbiano, G., & Elvis, M. 2001, *ApJL*, **552**, L109
- Merloni, A., & Fabian, A. C. 2001, *MNRAS*, **321**, 549
- Miller, J. M., Cackett, E. M., & Reis, R. C. 2009, *ApJL*, **707**, L77
- Miller, J. M., Fabbiano, G., Miller, M. C., & Fabian, A. C. 2003, *ApJL*, **585**, L37
- Miller, J. M., Fabian, A. C., & Miller, M. C. 2004, *ApJL*, **614**, L117
- Mitsuda, K., Inoue, H., Koyama, K., et al. 1984, *PASJ*, **36**, 741
- Pakull, M. W., & Mirioni, L. 2002, arXiv:astro-ph/0202488
- Pasham, D. R., & Strohmayer, T. E. 2013, *ApJ*, **764**, 93
- Paturel, G., Theureau, G., Fouque, P., et al. 2002, *A&A*, **383**, 398
- Pintore, F., & Zampieri, L. 2012, *MNRAS*, **420**, 1107
- Reis, R. C., Miller, J. M., Reynolds, M. T., et al. 2013, *ApJ*, **736**, 48
- Reynolds, M. T., & Miller, J. M. 2013, *ApJ*, **769**, 16
- Rykoff, E. S., Miller, J. M., Steeghs, D., & Torres, M. A. P. 2007, *ApJ*, **666**, 1129
- Salvesen, G., Miller, J. M., Reis, R. C., & Begelman, M. C. 2013, *MNRAS*, **431**, 3510
- Soria, R. 2007, *Ap&SS*, **311**, 213
- Swartz, D. A., Soria, R., Tennant, A. F., & Yukita, M. 2011, *ApJ*, **741**, 49
- Titarchuk, L. 1994, *ApJ*, **434**, 570
- Tully, R. B. 1988, *Nearby Galaxies Catalog* (Cambridge: Cambridge Univ. Press)
- Walton, D. J., Miller, J. M., Harrison, F. A., et al. 2013, *ApJL*, **773**, L9
- Walton, D. J., Miller, J. M., Reis, R. C., & Fabian, A. C. 2012, *MNRAS*, **426**, 473
- Winter, L. M., Mushotzky, R. F., & Reynolds, C. S. 2007, *ApJ*, **655**, 163